# Contact Doping with Sub-Monolayers of Strong Polyelectrolytes for Organic Photovoltaics

**ARTICLE** *in* ADVANCED ENERGY MATERIALS · SEPTEMBER 2014

Impact Factor: 16.15 · DOI: 10.1002/aenm.201400439



**14 AUTHORS**, INCLUDING:

Tomonori Saito
Oak Ridge National Laboratory
**49** PUBLICATIONS **931** CITATIONS
SEE PROFILE

Enrique Gomez
Pennsylvania State University
**77** PUBLICATIONS **1,651** CITATIONS
SEE PROFILE

# Contact Doping with Sub-Monolayers of Strong Polyelectrolytes for Organic Photovoltaics

*Gopal K. Mor, David Jones, Thinh P. Le, Zhengrong Shang, Patrick J. Weathers, Megumi K. B. Woltermann, Kiarash Vakhshouri, Bryan P. Williams, Sarah A. Tohran, Tomonori Saito, Rafael Verduzco, Alberto Salleo, Michael A. Hickner, and Enrique D. Gomez**

**Barriers to charge transfer at electrode-semiconductor contacts are ubiquitous and limit the applicability of organic semiconductors in electronic devices. Molecular or ionic doping near contacts can alleviate charge injection or extraction problems by enabling charge tunneling through contact barriers, but the soft nature of organic materials allows for small molecule dopants to diffuse and migrate, degrading the performance of the device and limiting effective interfacial doping. Here, it is demonstrated that contact doping in organic electronics is possible through ionic polymer dopants, which resist diffusion or migration due to their large size. Sub-monolayer deposition of non-conjugated strong polyelectrolytes, e.g., sulfonated poly(sulfone)s, at the anode-semiconductor interface of organic photovoltaics enables efficient hole extraction at the anode. The performance of contact-doped organic photovoltaics nearly matches the performance of devices composed of traditional hole transport layers such as poly(3,4-ethylenedioxythiophene):poly(styrene sulfonate) (PEDOT:PSS). The degree of sulfonation of the dopant polymer and the thickness of the ionic dopant layer is shown to be critical for optimizing doping and the efficiency of the device.**

## 1. Introduction

Electrode-semiconductor contacts in organic electronics are plagued by interfacial barriers for charge transfer due to poor alignment between the electrode work function and the Fermi level of the semiconductor, polarization or energetic disorder in the semiconductor near the electrode surface, and interfacial chemistry and structure.[1–5] Current approaches to making contacts are focused on tuning the work function of the electrode to match the transport level of the semiconductor,[6–11] even though polarization of the organic semiconductor at the interface often leads to ubiquitous contact barriers.[12–15] As a consequence, continued improvement in the performance of various organic electronic devices over the last few years continues due to the development of electrode and semiconducting materials without a clear picture of the factors affecting the electrode-semiconductor interface.[16–19]

Although making metal contacts to inorganic semiconductors share some of the same challenges as for organic semiconductors, effective contacts are made by heavily doping inorganic semiconductor-electrode interfaces and thereby enabling tunneling through thinned contact barriers.[20–22] Unfortunately, the open conformations and low density of organic materials enable small molecules to diffuse or migrate, limiting the applicability of contact doping to organic electronic devices. Furthermore, mobile ionic dopants will diffuse to build a concentration gradient in response to applied electric fields, effectively counteracting the field. For these reasons, contact-doping and fabricating efficient contacts remain a challenge in organic electronics.

An approach to address losses at electrode interfaces is to insert a carrier-specific transport layer in between electrodes

Dr. G. K. Mor, T. P. Le, P. J. Weathers, M. K. B. Woltermann, K. Vakhshouri, B. P. Williams, S. A. Tohran, Prof. E. D. Gomez
Department of Chemical Engineering,
The Pennsylvania State University
University Park, PA 16802, USA
E-mail: edg12@psu.edu

D. Jones, T. Saito, Prof. M. A. Hickner
Department of Materials Science and Engineering
The Pennsylvania State University
University Park, PA 16802, USA

Z. Shang, Prof. A. Salleo
Department of Materials Science and Engineering
Stanford University
Stanford, CA 94305, USA

Prof. R. Verduzco
Department of Chemical and Biomolecular Engineering
Rice University
Houston, TX 77005, USA

Prof. E. D. Gomez
Materials Research Institute
The Pennsylvania State University
University Park, PA 16802, USA

DOI: 10.1002/aenm.201400439

and the active layer. It is well-established that interfacial barriers at the indium tin oxide (ITO)-active layer interface limit the performance of organic photovoltaics and consequently the use of hole extraction layers at the anode are required for efficient device operation.[23–27] For example, poly(3,4-ethylenedioxythiophene):poly(styrenesulfonate) (PEDOT:PSS) was developed to facilitate charge injection into organic light emitting diodes[28–32] and was later utilized in the fabrication of organic solar cells. The role of hole transport layers has been hypothesized to be related to work function modification,[33–36] planarization,[37,38] and contact-doping.[39,40] Nevertheless, the design of novel or universal hole transport layers has been hampered due to the lack of basic knowledge identifying the functional mechanism by which materials such as PEDOT:PSS improve organic semiconductor-electrode contacts. Furthermore, materials such as PEDOT:PSS have their own intrinsic problems, such as acidity and hydrophilicity, which can compromise the stability of devices.

As an alternative to PEDOT:PSS, conjugated polyelectrolytes have been applied as interfacial layers to produce efficient organic solar cells.[41–43] The goal has been to design materials which are capable of creating interfacial dipoles at the electrode surface, thereby potentially modulating the work function of the electrode. This approach, however, does not address the inherent barriers (i.e., Schottky barriers) that can occur at contacts. Indeed, ultraviolet photoemission spectroscopy experiments have shown consistent contact barriers, of about 0.5 eV, between self-assembled monolayer-modified indium tin oxide electrodes and poly(3-hexylthiophene-2,5-diyl) despite variations of the electrode work function by 1.4 eV.[14]

Here, we demonstrate that by incorporating acidic dopant moieties into non-conjugated polymers we can achieve contact-doping in organic photovoltaics. Sulfonated poly(sulfone)s deposited at sub-monolayer coverages p-type-dope polymer donors in the active layer at the anode interface. Because the polymeric dopant resists diffusion or migration and is sequestered at the electrode-semiconductor interface, device performance that matches devices composed of standard hole transfer layers such as PEDOT:PSS is achieved. We hypothesize that our approach of doping the semiconductor layer near the electrode reduces the barrier thicknesses to enable carrier tunneling and achieve reduced contact resistances.

## 2. Results and Discussion

Polymeric dopants based on poly(sulfone) backbones were synthesized with varying degrees of sulfonation (**Figure 1**). We characterize the degree of sulfonation in terms of the equivalents of sulfonate groups per mass of polymer, or the ion exchange capacity (IEC). Each sulfonated poly(phenylsulfone) is labeled as SPS(x) where "x" is the IEC.

Polymers retain their bulk, unperturbed chain conformations even as film thicknesses decrease below the chain radius of gyration, such that ultra-thin films exhibit large surface roughness and incomplete surface coverage.[44,45] Thus, by depositing SPS from dilute polymer solutions onto indium tin oxide substrates, we can utilize the incomplete coverage of the electrode to create regions of the semiconductor which are both

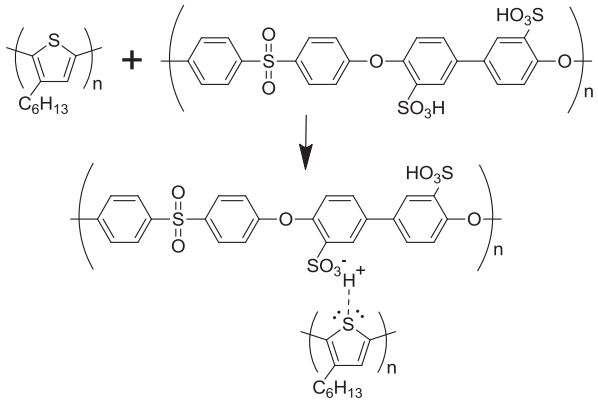


**Figure 1.** Chemical structure of P3HT and SPS. Proposed doping interaction between sulfonic acid groups of SPS and thiophene units of P3HT.

doped and also in contact with the electrodes. We deposit SPS films from solutions of 4:1 v:v chloroform:methanol at various polymer concentrations. Films cast at 0.15 mg $mL^{-1}$ are less than 3 nm thick (effective thickness, as measured by ellipsometry, Figure S1 of the Supporting Information), such that the UV-vis absorbance was negligible. For comparison, we estimate the radius of gyration of SPS to be 10 nm in the melt, much larger than the film thickness. Figure S2 of the Supporting Information shows scanning probe microscopy images of SPS films cast on ITO electrodes and Si wafers. As the solution concentration increases from 0.15 to 0.25 mg $mL^{-1}$, we observe more uniform films, suggesting incomplete coverage at low concentrations. Additionally, between 0.1 and 0.5 mg $mL^{-1}$, the plate-like structure of the ITO is readily visible and does not become planarized by the deposited polymer until a dopant solution concentration of 0.75 mg $mL^{-1}$. Thus, we surmise that at casting solution concentrations of SPS below 0.5 mg $mL^{-1}$, we have incomplete coverage of the ITO anode.

**Figure 2**a,b show the current-voltage characteristics of solar cells under AM 1.5G illumination (100 mW $cm^{-2}$) where the active layer is composed of either poly(3-hexylthiophene-2,5-diyl) (P3HT)/1′,1″,4′,4″-tetrahydro-di[1,4]methanonaphthaleno[1,2:2′,3′,56,60:2″,3″][5,6]-fullerene-$C_{60}$ (ICBA), or poly[*N*-9′-hepta-decanyl-2,7-carbazole-alt-5,5-(4′,7′-di-2-thienyl-2′,1′,3′-benzothiadiazole)] (PCDTBT)/[6,6]-phenyl-$C_{71}$-butyric acid methyl ester (PCBM). Treating ITO with the same solvents utilized to dissolve SPS had no effect on the performance of ITO-only devices. Devices with SPS at the anode interface show an increase in photoconversion efficiency as the IEC of SPS increases. Remarkably, devices made with SPS(2.3) as an interfacial layer perform similarly to devices utilizing PEDOT:PSS as a hole transport layer.

Figure 2c,d compare the device characteristics of devices made with bare ITO as the anode to devices made with varying amount of SPS(x) deposited at the ITO surface. The amount of SPS(x) is given in terms of the solution concentration prior to spin-coating. The average thickness of the thinnest layer of dopant polymer is estimated to be less than 3 nm from ellipsometry of films spin-coated on smooth Si substrates. As the amount of SPS increases, the overall performance of devices decreases. The open-circuit voltage of both P3HT/ICBA and

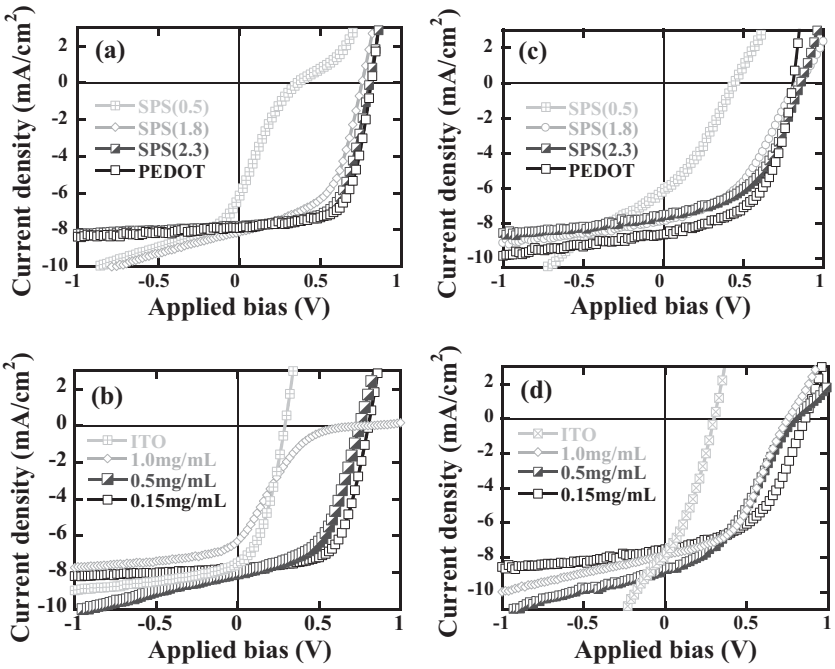


**Figure 2.** Current density vs. applied bias characteristics of P3HT/ICBA and PCDTBT:$PC_{71}BM$ based organic solar cells. a,b) Current-voltage characteristics for P3HT/ICBA devices with either SPS(0.5), SPS(1.8), SPS(2.3), ITO or PEDOT:PSS (PEDOT) as an interfacial layer at the anode. Panel (b) shows the dependence of device performance on SPS(2.3) solution concentration for P3HT/ICBA devices. c,d) Current-voltage characteristics for PCDTBT/$PC_{71}BM$ devices with either SPS(0.5), SPS(1.8), SPS(2.3), ITO or PEDOT:PSS as an interfacial layer at the anode. Panel (d) shows the dependence of device performance on SPS(2.3) solution concentration for PCDTBT/$PC_{71}BM$ devices.

PCDTBT/PCBM devices comprised of SPS(2.3) as an interfacial layer is greater than 0.8 V, while the short-circuit current for both set of devices is above 8 mA cm$^{-2}$. As the thickness of the SPS layer increases, current density–voltage (*J*–*V*) curves exhibit characteristics consistent with a blocking layer at one of the electrodes (Figure 2b,d). Such behavior is expected from thick, non-conducting SPS layers.

Figure 2 and Figure S3 of the Supporting Information show that the short-circuit current and open-circuit voltage of SPS-based devices quickly approach devices comprised of PEDOT:PSS as the sulfonation of SPS increases. The fill factor also increases with IEC of SPS, but more slowly than the other aforementioned device metrics. Thus, Figure S3 suggests that increasing the density of ionic groups in SPS beyond the materials in this study may continue to improve photovoltaic device performance.

A summary of performance in terms of the overall photoconversion efficiency for devices incorporating P3HT/ICBA or PCDTBT/PCBM in the active layer is shown in **Figure 3** as a function of the IEC for SPS. The performance of devices with PEDOT:PSS hole transport layers is also shown in Figure 3 as solid lines for the average efficiency and dotted lines for the standard deviation taken from multiple (at least six) devices. The overall performance increases for all cases with an increase in IEC of the SPS and approaches the performance of control devices composed of PEDOT:PSS. Devices incorporating SPS exhibit nearly 4% overall photoconversion efficiencies, a dramatic increase over devices with bare ITO anodes (efficiencies below 1%).

We explored the role that SPS has on the polymer donor by characterizing the thin-film transistor characteristics of devices where the active layer was composed of P3HT or PCDTBT mixed with SPS at varying concentrations. As shown in **Figure 4**, the off-current of P3HT and PCDTBT transistors increases by four to five orders of magnitude upon addition of SPS, suggesting that SPS dopes both P3HT and PCDTBT. We can estimate the number of carriers as the conductivity divided by the charge mobility extracted from the transistor characteristics at saturation. We obtain a carrier density of $3 \times 10^{17}$ cm$^{-3}$ for the highest concentration of SPS(2.3) in P3HT. Assuming a density of 1.33 g cm$^{-3}$, we estimate one charge per $2 \times 10^4$ rings.[46] Such carrier densities have been demonstrated to promote tunneling through barriers at contacts.[47,48]

We can confirm doping of P3HT and PCDTBT through UV-vis and photothermal deflection spectroscopy experiments. **Figure 5**a shows the absorption of P3HT and P3HT mixed with SPS(2.3), where an absorption feature is clearly visible near 1.25 eV for P3HT mixed with SPS(2.3). Doping of P3HT has been shown to produce an absorption feature near 1.25 eV (1000 nm) associated with the formation of polarons.[49–52] Figure 5b similarly demostrates the presence

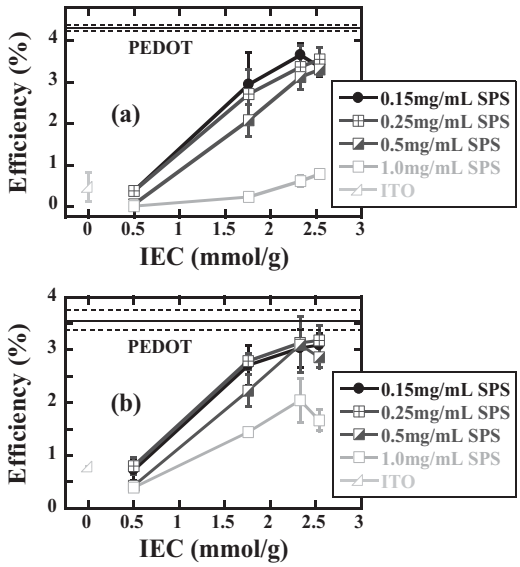


**Figure 3.** Solar cell efficiency vs. degree of sulfonation of SPS (IEC) for various SPS solution concentrations: a) P3HT/ICBA devices and b) PCDTBT/$PC_{71}BM$ solar cells. Device efficiencies for bare ITO and PEDOT:PSS coated ITO anodes are shown for comparison. The horizontal lines represent the efficiency values of PEDOT:PSS (PEDOT) devices. Error bars denote the standard deviation of data from multiple devices.

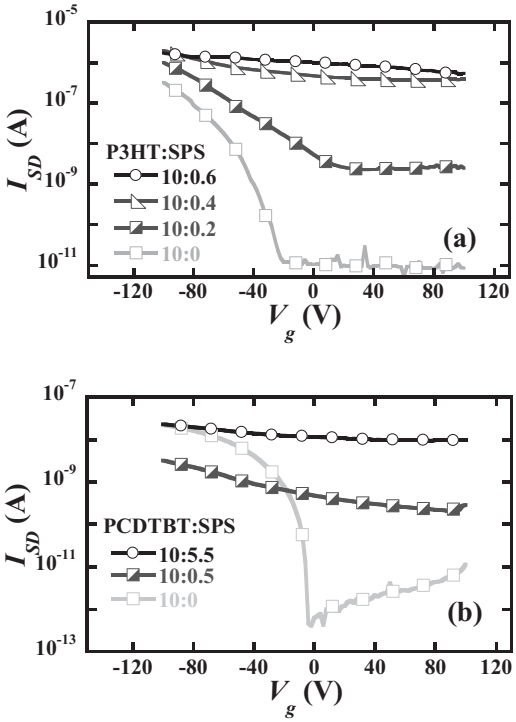


**Figure 4.** Transfer characteristics of a) P3HT:SPS(2.3) and b) PCDTBT:SPS(2.2) field-effect transistors taken at a source-drain voltage of –50 V. The solution concentrations were 10 mg mL$^{-1}$ for P3HT and 0.2, 0.4 or 0.6 mg mL$^{-1}$ for SPS(2.3) in (a) and 10 mg mL$^{-1}$ PCDTBT and 0.5 or 5.5 mg mL$^{-1}$ for SPS(2.2) in (b). Solutions were spin coated at 1000 RPM and then annealed at 150 °C for 10 min. Dielectric layers are 300 nm $SiO_2$ and the channel length and width are 20 and 220 μm, respectively.

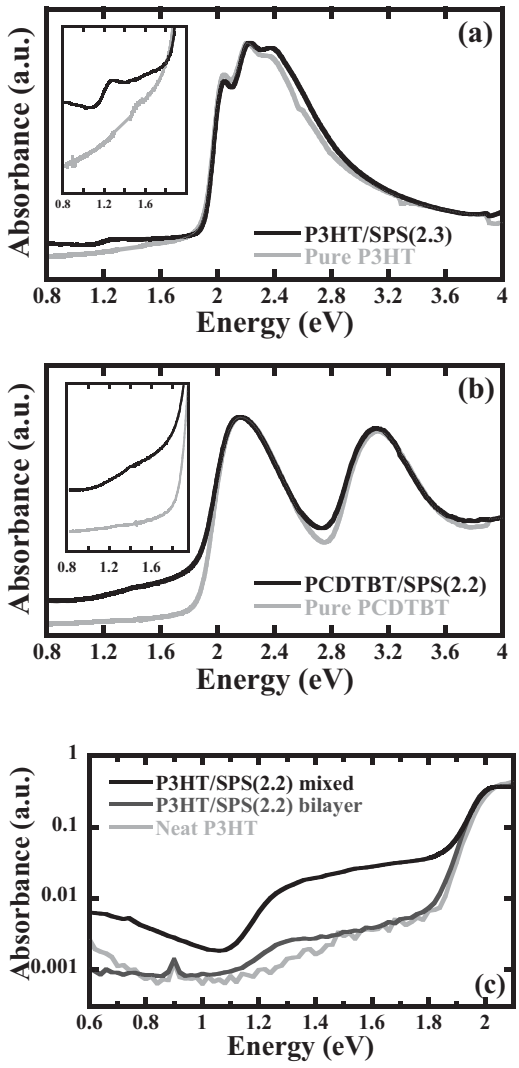


**Figure 5.** Normalized UV-Vis absorption spectra of a) P3HT and P3HT/SPS(2.3) mixtures and b) PCDTBT and PCDTBT/SPS(2.2) mixtures. Spectra were normalized by dividing by the largest absorbance value. A signature of polaron absorption is visible in the P3HT/SPS(2.3) mixture at about 1.25 eV (inset of a) and PCDTBT/SPS(2.2) mixture at 1.4 eV (inset of b), suggesting doping of P3HT by SPS(2.3) and PCDTBT by SPS(2.2). c) Photothermal deflection spectroscopy data of neat P3HT, P3HT/SPS(2.2) mixtures and P3HT/SPS(2.2) bilayers. Bilayers replicate the solar cell device architecture to demonstrate the presence of doped P3HT at the anodic interface.

of an absorption peak at 1.4 eV for PCDTBT mixed with SPS(2.2).

We can also take advantage of the enhanced sensitivity of photothermal deflection spectroscopy over UV-vis absorption experiments to obtain further evidence of doping at interfaces.[53,54] We deposited a layer of P3HT on top of SPS(2.2), in the same manner as devices are constructed. Thus, the feature at 1.25 eV in the PDS spectra shown in Figure 5c is indicative of doping of P3HT at the interface with SPS(2.2). We compare the PDS spectra of P3HT/SPS(2.2) bilayers to mixed films, where the peak at 1.25 eV is always visible and the low-energy polaron peak centered at 0.5 eV in P3HT is prominent (Figure 5c). The stronger evidence of doping in mixed films with respect to bilayers is likely due to mixing between P3HT and SPS(2.2), resulting in a larger interaction volume between the dopant polymer and P3HT.

The evidence of doping shown in Figure 4 and 5 implies that the effectiveness of SPS in promoting hole extraction at the anode is due to doping of thiophene rings at the semiconductor/ITO interface. Although doping at the anode/active layer interface of photovoltaic devices is not necessarily the same as bulk doping of P3HT transistor experiments, the charge carrier densities achievable in transistors via doping are in the $10^{17}$ cm$^{-3}$ range, suggesting that thinning of interfacial barriers at the anode contacts is possible. Based on our results, we propose a hypothesis for the role of PEDOT:PSS in solar cell or light-emitting devices: a critical interaction between PEDOT:PSS and the active layer of diode devices is the doping of the semiconductor layer by polystyrene sulfonate. Indeed, XPS results have shown that polystyrene sulfonate is found at the air surface of PEDOT:PSS films.[55–57] Thus, not only is the ability to dope the semiconductor active layer a critical parameter for the design of strong polyelectrolytes in hole extraction layers, the polyelectrolytes themselves could be utilized to contact-dope organic electronics at electrode interfaces.

## 3. Conclusions

In summary, we have demonstrated a general approach to achieve contact doping in organic diodes. The localization of polymeric strong acids to the anodic interface in photovoltaics leads to interfacial doping of conjugated polymers. Thus, we hypothesize that doping at the anode contact by sulfonated strong polyelectrolytes effectively thins the contact barriers which are responsible for poor charge extraction. The resulting device performance of organic photovoltaic devices incorporating ultra-thin polyelectrolytes as dopant layers matches that of devices comprised of PEDOT:PSS hole-extraction layers. We find that the number of sulfonate ions per dopant chain is critical to efficient charge extraction, suggesting that further engineering of the doping interaction between strongly acidic polyelectrolytes and conjugated polymers has the potential to further improve photovoltaic device efficiency.

## 4. Experimental Section

*Materials*: Poly(phenylsulfone) (Solvay Advanced Polymers, Radel R-5500, $M_W$ = 63 kg mol$^{-1}$, 2.5 g) was sulfonated by trimethylsilyl chlorosulfonate (Aldrich, 99%, $ClSO_3Si(CH_3)_3$_ in tetrachloroethane (Aldrich, 98%, 51 mL). A series of sulfonated Radel (S-Radel) was formed by stirring 1.0, 2.0, 4.0 and 5.5 N $ClSO_3Si(CH_3)_3$ in $C_2H_2Cl_4$ at 50 °C for two different reaction times 24 h and 96 h. The solution was then cooled to ambient temperature and poured into 50 mL methanol. The precipitated polymer was with methanol and later washed with water. The product was then dried under reduced pressure at 75 °C for 8 h. The degree of sulfonation (DS) per repeat unit and the corresponding ion exchange capacity (IEC) was determined using $^1$HNMR (Bruker-Spectrospin, 400MHz) after dissolving S-Radel in deuterated dimethyl sulfoxide (*d*-DMSO). Reaction conditions and properties of the four S-Radel samples are summarized in Supporting Information Table S1.[58] SPS(x) was used to denote specific samples where x indicates the IEC value. PCDTBT, $M_n$ = 20 to 100 kg mol$^{-1}$, was synthesized via Suzuki coupling.[59] 96% H-T regioregular P3HT with a number-average molecular weight of 28 kg mol$^{-1}$ and polydispersity index of 1.9 was purchased from Merck. PCBM was purchased from Nano-C and bisindene $C_{60}$ (ICBA) was purchased from Lumtec, Taiwan (>99% with isomers). PEDOT:PSS (Clevios P) was purchased from H.C. Starck. All purchased materials were used as received.

*Deposition of SPS(x) or PEDOT:PSS Layer*: SPS(x) was weighed in air and dissolved in a 4:1 by volume anhydrous chloroform/methanol solution in a $N_2$-filled glove box (MBraun) at four different concentrations (0.15, 0.25, 0.5 and 1.0 mg mL$^{-1}$). Solutions were aged for 48 h without stirring. Patterned ITO-coated glass (20 Ω/square, Xin Yan, Hong Kong) was cleaned with a non-ionic detergent (Aquet), thoroughly rinsed with 18.5 MΩ cm water, and ultrasonicated in acetone and isopropanol for 10 min each. Finally, substrates were exposed to UV-ozone for 10 min immediately prior to deposition of SPS(x) or PEDOT:PSS. SPS(x) solutions were spun cast at 4000 rpm for 60 s on the cleaned ITO-coated glass inside the $N_2$ glove box. Samples were then dried for 4 min at room temperature prior to deposition of the organic donor/acceptor layer. PEDOT:PSS solutions were filtered through a 0.45 µm PVDF syringe filter and spun cast on the ITO substrates at 4000 rpm for 120 s. Films were subsequently heated at 165 °C for 10 min in air. The thickness of the resulting PEDOT layer was about 70 nm. Samples were then immediately transferred into the glove box for donor/acceptor layer deposition.

*Deposition of P3HT/ICBA Layer*: 1:1 by mass P3HT/ICBA mixtures were made by dissolution in anhydrous *o*-dichlorobenzene (Sigma Aldrich) inside a $N_2$ glove box at 35 mg mL$^{-1}$. Solutions were stirred at 60 °C for 20 h. The temperature of the polymer solution was raised to 70 °C for 30 min prior to use. Solutions were spun cast at 1000 rpm for 30 s on SPS(x)- or PEDOT-coated ITO substrates. Wet films were immediately covered by a glass petri dish. After self-drying of the polymer film for about 30 min, samples were annealed at 150 °C for 10 min and rapidly cooled to room temperature by placing them on a room-temperature metal surface.

*Deposition of PCDTBT/PCBM Layer*: PCDTBT and PCBM at a 1:4 by mass ratio were dissolved in anhydrous *o*-dichlorobenzene at 35 mg mL$^{-1}$. Solutions were stirred on a hot plate set at 65 °C for 20 h. The temperature of the solution was decreased to 55 °C and held for 45 min before film casting. Polymer solutions were spun cast at 2000 rpm for 60 s on SPS(x)- or PEDOT-coated ITO glass. Samples were then annealed at 70 °C for 1 h inside a covered glass petri dish and then immediately cooled to room temperature by quenching on a metal surface.

*Deposition of Ca/Al Cathode*: Ca and Al layers were thermally evaporated on the P3HT/ICBA and PCDTBT/PCBM active layers to complete devices. Ca (≈20 nm) was deposited at a rate of 0.4–0.8 Å s$^{-1}$ followed by Al (≈70 nm) at a rate of 0.4–1.5 Å s$^{-1}$. The evaporator pressure was $1 \times 10^{-6}$ mbar. Each ITO electrode chip contains six subcells each with an active area of 0.162 cm$^2$.

*J-V Characteristics Measurements*: Solar cells were tested inside the $N_2$-filled glove box under AM 1.5 G 100 mW cm$^{-2}$ illumination and in the dark. The lamp intensity was verified with a thermopile power meter and an NREL certified Si reference cell (Newport). Current-voltage characteristics were measured using a Labview-controlled Keithley 2636A source meter. All processing and device testing was carried out in a $N_2$ glove box without sample transfer to the ambient.

*OFET Fabrication and Testing*: Heavily doped p-type silicon wafers with a 300 nm thick thermal oxide layers ($C_{ox}$ = 10.6 nF cm$^{-2}$) were used as the gate electrode and dielectric. Gold source/drain electrodes with thicknesses of approximately 100 nm were patterned through conventional double-layer lithography on the $SiO_2$ wafers. After gold electrode deposition, the $SiO_2$ surface was coated with hexamethyldisilazane (HMDS, >99%, Sigma Aldrich) by spin-coating at 4000 rpm for 30 s. The resulting bottom-contact, bottom-gate FET devices have a channel length and channel width of 20 µm and 220 µm, respectively. Mixtures with varying composition of P3HT/SPS(2.3) were made by dissolution in 1:4 v:v methanol/chloroform mixtures at varying amount of solids. P3HT/SPS(2.3) solutions were spun cast at 1000 rpm for 60 s on the HMDS-treated $SiO_2$ substrate. Samples were then heated to 150 °C for 10 min. Electrical characterization was conducted with a Labview-controlled Keithley 2636A system source meter. All processing and device testing was carried out in a $N_2$ glove box without ambient sample exposure.

*UV-Vis-NIR Absorption Measurements*: Optical absorption measurements were performed to analyze the doping of P3HT by SPS(2.3) through examining the free carrier tail in the long wavelength range. P3HT and SPS(2.3) were dissolved at 1.0 mg and 0.257 mg, respectively, to create a 10:1 ratio between P3HT repeat untis and sulfonic acid groups on the SPS(2.3). Solvent containing a 12:3:1 volume ratio of chlorobenzene:chloroform:methanol was added to dissolve the dry 1.0 mg of P3HT and 0.257 mg of SPS(2.3) and then the solution was stirred continuously in a glove box for 48 h. The solution was then drop cast on a KBr pellet and dried for 1 h before it was removed from the glove box and immediately tested in atmosphere. A Perkin Elmer Lambda 950 UV-Vis NIR spectrometer was used to measure optical absorption of the doped P3HT film both as-cast and after annealing at 150 °C for 10 min. The optical absorption spectrum of an undoped P3HT film was taken under the same conditions as a reference.

*Photothermal Deflection Spectroscopy*: Samples were spin-coated on quartz substrates. The PDS set-up used chopped (3.333Hz) monochromatic light from a 100 W halogen lamp as the pump light. The sample was immersed in a liquid deflection medium perfluorohexane ($C_6F_{14}$, 3 M Fluorinert FC-72). A HeNe laser (633 nm) beam perpendicular to the pump light passed through the deflection medium near the surface of the sample film, whose deflection was recorded by a position-sensitive Si detector. The detector was connected to a Stanford Research System SR380 lock-in amplifier.

## Supporting Information

Supporting Information is available from the Wiley Online Library or from the author.

## Acknowledgements

Funding support from NSF under Award CBET-1067470 is acknowledged.

Received: March 12, 2014
Revised: April 10, 2014
Published online:

[1] C. Vanoni, S. Tsujino, T. A. Jung, *Appl. Phys. Lett.* **2007**, *90*, 193119.
[2] J. Hwang, A. Wan, A. Kahn, *Mater. Sci. Eng. R.* **2009**, *64*, 1.
[3] D. Cahen, A. Kahn, *Adv. Mater.* **2003**, *15*, 271.
[4] D. J. Gundlach, L. L. Jia, T. N. Jackson, *IEEE Electron Dev. Lett.* **2001**, *22*, 571.
[5] D. J. Gundlach, L. Zhou, J. A. Nichols, T. N. Jackson, P. V. Necliudov, M. S. Shur, *J. Appl. Phys.* **2006**, *100*, 024509.
[6] C. Uhrich, R. Schueppel, A. Petrich, M. Pfeiffer, K. Leo, E. Brier, P. Kilickiran, P. Baeuerle, *Adv. Funct. Mater.* **2007**, *17*, 2991.
[7] C. J. Brabec, A. Cravino, D. Meissner, N. S. Sariciftci, M. T. Rispens, L. Sanchez, J. C. Hummelen, T. Fromherz, *Thin Solid Films* **2002**, *403*, 368.
[8] H. Frohne, S. E. Shaheen, C. J. Brabec, D. C. Muller, N. S. Sariciftci, K. Meerholz, *ChemPhysChem* **2002**, *3*, 795.
[9] E. D. Gomez, Y.-L. Loo, *J. Mater. Chem.* **2010**, *20*, 6604.
[10] B. H. Hamadani, D. A. Corley, J. W. Ciszek, J. M. Tour, D. Natelson, *Nano Lett.* **2006**, *6*, 1303.
[11] G. Heimel, L. Romaner, E. Zojer, J. L. Bredas, *Nano Lett.* **2007**, *7*, 932.
[12] K. P. Puntambekar, P. V. Pesavento, C. D. Frisbie, *Appl. Phys. Lett.* **2003**, *83*, 5539.
[13] X. Crispin, V. Geskin, A. Crispin, J. Cornil, R. Lazzaroni, W. R. Salaneck, J. L. Bredas, *J. Am. Chem. Soc.* **2002**, *124*, 8131.
[14] H. Wang, E. D. Gomez, Z. Guan, C. Jaye, M. F. Toney, D. A. Fischer, A. Kahn, Y.-L. Loo, *J. Phys. Chem. C* **2013**, *117*, 20474.
[15] J. A. Nichols, D. J. Gundlach, T. N. Jackson, *Appl. Phys. Lett.* **2003**, *83*, 2366.
[16] V. Shrotriya, G. Li, Y. Yao, C. W. Chu, Y. Yang, *Appl. Phys. Lett.* **2006**, *88*, 073508.
[17] M. D. Irwin, B. Buchholz, A. W. Hains, R. P. H. Chang, T. J. Marks, *Proc. Natl. Acad. Sci. USA* **2008**, *105*, 2783.
[18] S. Han, W. S. Shin, M. Seo, D. Gupta, S. J. Moon, S. Yoo, *Org. Electron.* **2009**, *10*, 791.
[19] N. Li, B. E. Lassiter, R. R. Lunt, G. Wei, S. R. Forrest, *Appl. Phys. Lett.* **2009**, *94*, 023307.
[20] R. V. Ghita, C. Logofatu, C. Negrila, A. S. Manea, M. Cernea, M. F. Lazarescu, *J. Optoelectron. Adv. Mater.* **2005**, *7*, 3033.
[21] S. M. Sze, *Semiconductor Devices: Physics and Technology*, John Wiley and Sons, Inc., New York **2002**.
[22] A. G. Baca, F. Ren, J. C. Zolper, R. D. Briggs, S. J. Pearton, *Thin Solid Films* **1997**, *308*, 599.
[23] J. E. Yoo, K. S. Lee, A. Garcia, J. Tarver, E. D. Gomez, K. Baldwin, Y. M. Sun, H. Meng, T. Q. Nguyen, Y. L. Loo, *Proc. Natl. Acad. Sci. USA* **2010**, *107*, 5712.
[24] S. H. Oh, S. I. Na, J. Jo, B. Lim, D. Vak, D. Y. Kim, *Adv. Funct. Mater.* **2010**, *20*, 1977.
[25] L.-M. Chen, Z. Xu, Z. Hong, Y. Yang, *J. Mater. Chem.* **2010**, *20*, 2575.
[26] R. Steim, F. R. Kogler, C. J. Brabec, *J. Mater. Chem.* **2010**, *20*, 2499.
[27] C. He, C. M. Zhong, H. B. Wu, R. Q. Yang, W. Yang, F. Huang, G. C. Bazan, Y. Cao, *J. Mater. Chem.* **2010**, *20*, 2617.
[28] C. Jonda, A. B. R. Mayer, U. Stolz, A. Elschner, A. Karbach, *J. Mater. Sci.* **2000**, *35*, 5645.
[29] S. A. Carter, M. Angelopoulos, S. Karg, P. J. Brock, J. C. Scott, *Appl. Phys. Lett.* **1997**, *70*, 2067.
[30] J. C. Scott, S. A. Carter, S. Karg, M. Angelopoulos, *Synth. Met.* **1997**, *85*, 1197.
[31] A. Berntsen, Y. Croonen, C. Liedenbaum, H. Schoo, R. J. Visser, J. Vleggaar, P. van de Weijer, *Opt. Mater.* **1998**, *9*, 125.
[32] A. Elschner, F. Bruder, H. W. Heuer, F. Jonas, A. Karbach, S. Kirchmeyer, S. Thurm, *Synth. Met.* **2000**, *111*, 139.
[33] T. M. Brown, J. S. Kim, R. H. Friend, F. Cacialli, R. Daik, W. J. Feast, *Appl. Phys. Lett.* **1999**, *75*, 1679.
[34] F. Zhang, A. Petr, H. Peisert, M. Knupfer, L. Dunsch, *J. Phys. Chem.* **2004**, *108*, 17301.
[35] *Organic Photovoltaics: Materials, Device Physics, and Manufacturing Technologies*, (Ed: C. Brabec, U. Scherf, V. Dyakonov), Wiley-VCH, Weinheim, Germany **2008**.
[36] J. Luo, H. B. Wu, C. He, A. Y. Li, W. Yang, Y. Cao, *Appl. Phys. Lett.* **2009**, *95*, 043301.
[37] G. Wantz, L. Hirsch, N. Huby, L. Vignau, J. F. Silvain, A. S. Barriere, J. P. Parneix, *Thin Solid Films* **2005**, *485*, 247.
[38] S. J. Chua, L. Ke, R. S. Kumar, K. Zhang, *Appl. Phys. Lett.* **2002**, *81*, 1119.
[39] J. M. Bharathan, Y. Yang, *J. Appl. Phys.* **1998**, *84*, 3207.
[40] K. Book, H. Bassler, A. Elschner, S. Kirchmeyer, *Org. Electron.* **2003**, *4*, 227.
[41] J. H. Seo, A. Gutacker, Y. M. Sun, H. B. Wu, F. Huang, Y. Cao, U. Scherf, A. J. Heeger, G. C. Bazan, *J. Am. Chem. Soc.* **2011**, *133*, 8416.
[42] Z. C. He, C. M. Zhong, S. J. Su, M. Xu, H. B. Wu, Y. Cao, *Nat. Photonics* **2012**, *6*, 591.
[43] H. Wu, F. Huang, J. Peng, Y. Cao, *Org. Electron.* **2005**, *6*, 118.
[44] R. L. Jones, S. K. Kumar, D. L. Ho, R. M. Briber, T. P. Russell, *Nature* **1999**, *400*, 146.
[45] R. L. Jones, S. K. Kumar, D. L. Ho, R. M. Briber, T. P. Russell, *Macromolecules* **2001**, *34*, 559.
[46] M. M. Erwin, J. McBride, A. V. Kadavanich, S. J. Rosenthal, *Thin Solid Films* **2002**, *409*, 198.
[47] I. D. Parker, *J. Appl. Phys.* **1994**, *75*, 1656.
[48] D. Neamen, *Semiconductor Physics and Devices*, McGraw-Hill, New York, NY **2002**.
[49] J. M. Guo, H. Ohkita, H. Benten, S. Ito, *J. Am. Chem. Soc.* **2009**, *131*, 16869.
[50] O. J. Korovyanko, R. Osterbacka, X. M. Jiang, Z. V. Vardeny, R. A. J. Janssen, *Phys. Rev. B* **2001**, 64.
[51] X. M. Jiang, R. Osterbacka, O. Korovyanko, C. P. An, B. Horovitz, R. A. J. Janssen, Z. V. Vardeny, *Adv. Funct. Mater.* **2002**, *12*, 587.
[52] R. Osterbacka, C. P. An, X. M. Jiang, Z. V. Vardeny, *Science* **2000**, *287*, 839.
[53] A. C. Boccara, D. Fournier, W. Jackson, N. M. Amer, *Opt. Lett.* **1980**, *5*, 377.
[54] C. H. Peters, I. T. Sachs-Quintana, W. R. Mateker, T. Heumueller, J. Rivnay, R. Noriega, Z. M. Beiley, E. T. Hoke, A. Salleo, M. D. McGehee, *Adv. Mater.* **2012**, *24*, 663.
[55] G. Greczynski, T. Kugler, M. Keil, W. Osikowicz, M. Fahlman, W. R. Salaneck, *J. Electron Spectrosc. Relat. Phenom.* **2001**, *121*, 1.
[56] G. Greczynski, T. Kugler, W. R. Salaneck, *Thin Solid Films* **1999**, *354*, 129.
[57] J. Hwang, F. Amy, A. Kahn, *Org. Electron.* **2006**, *7*, 387.
[58] T. Saito, M. D. Merrill, V. J. Watson, B. E. Logan, M. A. Hickner, *Electrochim. Acta* **2010**, *55*, 3398.
[59] N. Blouin, A. Michaud, M. Leclerc, *Adv. Mater.* **2007**, *19*, 2295.